Hedgehog signaling is required for cranial neural crest morphogenesis and chondrogenesis at the midline in the zebrafish skull

Naoyuki Wada[1], Yashar Javidan[1], Sarah Nelson[1], Thomas J. Carney[2], Robert N. Kelsh[2] and Thomas F. Schilling[1,*]

[1]Department of Developmental and Cell Biology, University of California, Irvine, 5210 McGaugh Hall, Irvine, CA 92697-2300, USA
[2]Centre for Regenerative Medicine, Developmental Biology Programme, School of Biology and Biochemistry, University of Bath, Bath BA2 7AY, UK
*Author for correspondence (e-mail: tschilli@uci.edu)

Accepted 16 June 2005

Development 132, 3977-3988
Published by The Company of Biologists 2005
doi:10.1242/dev.01943

Summary

Neural crest cells that form the vertebrate head skeleton migrate and interact with surrounding tissues to shape the skull, and defects in these processes underlie many human craniofacial syndromes. Signals at the midline play a crucial role in the development of the anterior neurocranium, which forms the ventral braincase and palate, and here we explore the role of Hedgehog (Hh) signaling in this process. Using *sox10:egfp* transgenics to follow neural crest cell movements in the living embryo, and vital dye labeling to generate a fate map, we show that distinct populations of neural crest form the two main cartilage elements of the larval anterior neurocranium: the paired trabeculae and the midline ethmoid. By analyzing zebrafish mutants that disrupt *sonic hedgehog* (*shh*) expression, we demonstrate that *shh* is required to specify the movements of progenitors of these elements at the midline, and to induce them to form cartilage. Treatments with cyclopamine, to block Hh signaling at different stages, suggest that although requirements in morphogenesis occur during neural crest migration beneath the brain, requirements in chondrogenesis occur later, as cells form separate trabecular and ethmoid condensations. Cell transplantations indicate that these also reflect different sources of Shh, one from the ventral neural tube that controls trabecular morphogenesis and one from the oral ectoderm that promotes chondrogenesis. Our results suggest a novel role for Shh in the movements of neural crest cells at the midline, as well as in their differentiation into cartilage, and help to explain why both skeletal fusions and palatal clefting are associated with the loss of Hh signaling in holoprosencephalic humans.

Key words: Craniofacial, Cleft palate, Neural crest, Holoprosencephaly, *Danio rerio*

Introduction

Cranial neural crest (NC) cells in the vertebrate embryo form most of the cartilage and bones of the skull. The head skeleton has a mediolateral (ML) polarity. Some skeletal elements form singly, at the midline, whereas others develop bilaterally at different distances on either side (De Beer, 1937). Fate-mapping studies of NC in embryos of fish, amphibians, birds and mammals have all shown that streams of NC cells from the hindbrain form most of the pharyngeal skeleton or 'viscerocranium', while more anterior NC cells form the braincase or 'neurocranium' (Horstadius and Sellman, 1946; Chibon, 1967; Le Lievre, 1978; Couly et al., 1993; Lumsden et al., 1993; Schilling and Kimmel, 1994; Osumi-Yamashita et al., 1994). These NC cells carry intrinsic differences acquired prior to migration that influence their skeletal fates along the anteroposterior (AP) axis (Noden, 1983; Trainor and Krumlauf, 2002), but also require inductive signals from surrounding endoderm and ectoderm (Hall, 1980; Couly et al., 2002; David et al., 2002; Crump et al., 2004a; Crump et al., 2004b; Le Douarin et al., 2004). Many studies have addressed the roles of these signals in AP patterning, but less is known about how skeletal polarity is established along the ML axis.

The anterior neurocranium (ANC) of larval zebrafish consists of paired trabecular rods joined at the midline anteriorly to form the ethmoid plate (Fig. 1A), and these form a striking example of M-L polarity. Genetic studies in zebrafish and mice have revealed that one member of the Hedgehog family of secreted proteins expressed at the midline, Sonic hedgehog (Shh), is required for ANC formation. Hh proteins act as polarizing factors in other contexts. *Shh* is expressed in the midline prechordal plate mesoderm and floorplate of the CNS adjacent to NC progenitors of the ANC (Strahle et al., 2004). Inactivation of zebrafish *shh* or other components of its signal transduction pathway causes ML patterning defects in which trabecular cartilages fuse at the midline, which is consistent with *shh* having a role in polarity (Brand et al., 1996; Schilling, 1997; Kimmel et al., 2001). Similarly, loss-of-function mutations in *Shh* in the mouse cause severe defects in cranial growth and loss of virtually all of the craniofacial bones (Chiang et al., 1996). Humans with mutant *SHH* exhibit

holoprosencephaly (HPE), often accompanied by midline craniofacial defects and palatal clefting (Gorlin et al., 1990; Roessler et al., 1996; Muenke and Beachy, 2000). Recent studies in mice have also shown that NC cells require the essential Hh receptor co-factor Smoothened (Smo) for craniofacial development, suggesting that Shh acts directly on skeletal progenitors (Jeong et al., 2004). Given its well-established role in regulating polarity in the neural tube and limb bud in a concentration-dependent manner (Ingham and McMahon, 2001), Shh is a good candidate for a signal in the NC environment that polarizes skeletal fates along the ML axis. In zebrafish, *shh* may share this role with its close relative *tiggy-winkle hedgehog* (*twhh*), which is expressed in a similar pattern.

Shh is expressed in several craniofacial tissues, including the early embryonic mesendoderm, ventral brain and oral ectoderm, and one or more of these sources could mediate its roles in ANC patterning. Surgical removal of oral ectoderm causes midfacial clefting in chicken embryos, whereas exogenous SHH protein causes midfacial expansion and, in some cases, duplications of midline structures of the ANC such as the nasal bone (Helms et al., 1997; Hu and Helms, 1999; Hu et al., 2003). These and other results have implicated Hh signaling from the facial ectoderm in ML patterning of the face, and in the regulation of NC proliferation and/or survival (Ahlgren et al., 2002). Endodermal expression of *Shh* is less important in this process, as zebrafish mutants that eliminate endoderm, such as *casanova*, lack viscerocranial cartilages but still form an ANC (David et al., 2002). Thus, *Shh* from the oral ectoderm may play a crucial role in ML polarity that is conserved in all vertebrates. However, the precise source of the Hh that controls facial patterning remains unclear.

Here, we present a characterization of NC morphogenesis and skeletal patterning in the *sonic you* (*syu*) mutant zebrafish, which disrupts the *shh* gene, and in embryos treated with the Hh inhibitor cyclopamine (CyA), at different stages of NC development. By constructing a transgenic line in which NC cells fluoresce in the living embryo, we are able for the first time to follow their migratory pathways in detail. We show that two distinct groups of NC form the trabecular and medial ethmoid cartilages of the ANC, contrary to the classical notion that the ethmoid simply forms by trabecular fusion. Both sets of NC cells require Hh signaling, but we argue that they do so at different times and in different regions, and that this helps to explain the spectrum of ML polarity defects observed in fish, mice and humans that are mutant in the Hh pathway. We suggest that Hh signals act both early, to separate skeletogenic NC at the midline, and later, to promote chondrogenesis, and that multiple sources of Shh induce the final skeletal pattern.

Materials and methods

Zebrafish lines

Zebrafish embryos were obtained in natural crosses and staged as previously reported (Kimmel et al., 1995). The AB strain was used as wild type. *sox10:egfp* transgenic fish [Tg(–4.9*sox10:egfp*)^{ba2}], which express *egfp* under the control of the *sox10*-promoter, were generated by microinjection of a DNA construct containing 4.9 kb of upstream sequence at the one-cell stage (T.J.C. and R.N.K., unpublished). Homozygous *sonic you* (*syu*^{tq252}) and *slow muscle omitted* (*smu*^{b641}) mutants were isolated from their siblings by somite morphology at 20 hours post-fertilization (hpf) (van Eeden et al., 1996; Schuarte et al., 1998; Varga et al., 2001).

Morpholinos

Morpholinos targeting zebrafish *shh* (*shh*-MO) and *tiggy-winkle hedgehog* (*twhh*-MO) were obtained (GeneTools) as reported previously (Nasevicius and Ekker, 2000). These were microinjected at the one- to two-cell stage, either alone or in combination. Defects depended on the amount of MO injected; for most experiments, we injected 2.0 ng *shh*-MO and 0.55 ng *twhh*-MO (Fig. 1).

Phenotypic analysis

For skeletal analysis, larvae were fixed at 4-5 dpf and stained for cartilage with Alcian Blue, after which they were dissected and flat-mounted as described (Javidan and Schilling, 2004). In situ hybridization was performed as described previously (Thisse et al., 1993). Probes used in this study were *foxd3* (Odenthal and Nusslein-Volhard, 1998), *shh* (Krauss et al., 1993), *ptc1* (Concordet et al., 1996), *sox9a* (Yan et al., 2002) and *sox10* (Dutton et al., 2001).

Confocal imaging

For live imaging of NC, heterozygous *sox10:egfp*$^{+/–}$ embryos (homozygous embryos showed variable defects in NC survival), were dechorionated at 12 hpf and mounted in 0.75% agarose on bridged coverslips. To prevent drying, petroleum jelly (Vaseline) was used to form a chamber of embryo medium containing tricaine anaesthetic, and this was sealed with a second coverslip. Time-lapsed imaging was performed using a Zeiss LSM 510 laser confocal microscope at 10 minute intervals. At each time point, approximately 100-μm *z*-stacks at 5 μm intervals were captured. Movies of projected *z*-stacks, as well as individual *z*-sections, were configured and individual cells followed manually. To analyze the later distribution of *egfp*+ cells, embryos were fixed with 4% paraformaldehyde (PFA) for 8 hours at 4°C, washed several times with PBS, and embedded in 1.5% agar after manual yolk removal. Images were captured at 2 μm intervals.

Cell labeling and fate mapping

Premigratory and postmigratory NC in *sox10:egfp* fish were labeled with either the lipophilic fluorescent dye, PKH26 (Sigma), or by intracellular microinjection of TRITC-dextran (Molecular Probes, #1817) into single cells. The distribution of their descendants was determined in the ANC 2-3 days later. Anesthetized embryos were mounted in 3% methylcellulose and a small volume of PKH-solution (20% in dilution solution) was injected through a small cut in the surface ectoderm made with a tungsten needle. On average, this labeled five to ten cells. Injection sites were recorded and the embryos subsequently raised until 80-85 hpf, when they were fixed in PFA for 8-12 hours, dissected and flat-mounted for observation of PKH+ cells.

Intracellular, single-cell labeling with tetramethylrhodamine-dextran (TRITC-dextran; 10,000 MW) was performed by iontophoresis, as previously reported (Schilling and Kimmel, 1994). Briefly, dechorionated embryos were mounted in 1.5% agar, agar was removed adjacent to the injection site and TRITC (3% in 0.2 M KCl) was injected iontophoretically; fluorescence was monitored continuously on a Zeiss Axioplan2 fluorescence microscope. Injection sites were recorded within 1 hour after injection, and the embryos were incubated for another 2-3 days to analyze cartilage.

Cyclopamine treatments

A 10 mM stock solution of cyclopamine (CyA), dissolved in 95% methanol, was diluted in embryo medium to different concentrations between 5-100 μM. Embryos were soaked in CyA solutions at different stages between 0-48 hpf, washed several times in embryo medium, and either fixed at 24-36 hpf for in situ hybridization for *ptc1* or raised for another 2-3 days for Alcian staining.

mRNA injections and bead implantation

Shh was overexpressed by injecting 0.3 ng of zebrafish *shh* mRNA into embryos at the 1-2 cell stage. For misexpression experiments at later stages, beads coated in recombinant Shh protein were implanted.

CM-AffiGel Blue beads (70-100 μm diameter, Bio-Rad) were incubated in Shh protein (mouse recombinant, 10 μg/ml, R&D Systems) at 4°C for 1 hour. Using a tungsten needle, a small slit was made posterior to the left eye. A protein-coated bead was inserted, and positioned between eye and brain (see Fig. 7C inset). Control beads were coated in 0.1% BSA-PBS. Treated embryos were incubated and fixed for cartilage analysis.

Cell transplantation

Wild-type donors were injected at the one- to two-cell stage with a mixture of 3% TRITC-dextran and 3% biotinylated-dextran, and cells were transplanted into *syu*^{tq252} mutants (or *shh*-MO/*twhh*-MO-injected embryos). Transplants were either placed near the animal pole to target surface ectoderm, or further vegetally to target the ventral brain in these experiments. Donors for ventral brain transplants were injected with small amounts of Taram-A (Tar*; 0.5 ng/embryo), which biases them toward dorsal fates, including floorplate. At 24 hpf, the positions of fluorescent donor cells were recorded and then embryos were raised to 4 dpf for skeletal analysis. Biotin-labeled donor cells were detected with a Vectastain Elite ABC kit (Vectastain) and DAB as the substrate.

Results

Hh signaling is essential for development of the anterior neurocranium

Loss of Shh function in the *sonic you* (*syu*^{tq252}) mutant causes variable midline defects and fusions of trabeculae in the ANC (Fig. 1A-C). To address redundant functions of the two closely related Hh-family members *shh* and *twhh* in the ANC, we used antisense morpholino oligonucleotides (MOs) to inhibit their translation. Both are expressed at the midline in zebrafish and are partially redundant in patterning of the neural tube (Ekker et al., 1995). Co-injection of the *shh*-MO and *twhh*-MO (hereafter referred to as 'Hh-deficient') caused midline ANC fusions in a concentration-dependent manner (Fig. 1D-F). Injections of 3 ng/embryo or more led to severe shortening or loss of trabeculae (Fig. 1D), whereas injections of 2 ng/embryo or less caused midline fusions similar to those seen in *syu* mutants (Fig. 1E). A complete loss of Hh signaling, as seen in the *smooth muscle omitted* (*smu*^{b641}) mutant, eliminates the neurocranium altogether (data not shown) (Chen et al., 2001; Varga et al., 2001).

To determine the stage at which cranial cartilage formation is disrupted in Hh-deficient embryos, we first analyzed chondrogenesis with Alcian staining. In wild types, trabecular cartilage is first detected between 45-48 hpf (Schilling and Kimmel, 1997). Two parallel, single-cell rows of chondrocytes form between the eyes (Fig. 2A), and these fuse in the midline at their anterior ends to form the ethmoidal plate by 56 hpf (Fig. 2B,C). At the same time, the trabeculae elongate rapidly and their posterior ends fuse to the basal plate of the skull (Fig. 2B-D). To examine pre-chondrogenic cells of the ANC in wild type, we analyzed expression of the Sox transcription factor *sox9a* during NC migration and condensation beneath the brain (Fig. 2I-L). Expression of *sox9a* mRNA is first detected at 24 hpf (data not shown), and by 30 hpf marks bilateral clusters of cells between the diencephalon and the eyes (Fig. 2I). These elongate by 36 hpf to prefigure the trabeculae (Fig. 2J). Expression of *sox9a* in ethmoid progenitors is first detected at 42 hpf, and these bridge the anterior ends of the trabecular condensations by 45 hpf (Fig. 2K).

In contrast to wild type, the first chondrocytes detected between the eyes in *syu* mutants lie further posteriorly, in small clusters near the anterior end of the notochord. These fuse at the midline to form a single rod of cartilage that bifurcates at its posterior end (Fig. 2E-H). *sox9a* expression in mutant ANC precursors is delayed compared with wild type (Fig. 2M), but by 36 hpf expression reveals fused condensations that form the ANC, ~10 hours prior to differentiating as cartilage (Fig. 2N). Thus, the fusions of trabecular cartilages in *syu* homozygous larvae result from an earlier NC defect.

Following skeletal precursors in NC with *sox10:egfp*

Cartilage fusions at the midline in *syu* mutants could be due to abnormal NC migration or later ectopic fusions of NC streams after their migration beneath the brain. To distinguish between these possibilities, we followed cranial NC morphogenesis in wild-type and Hh-deficient embryos using a newly generated transgenic line in which 4.9 kb of the *sox10* promoter drives *egfp* expression in NC. A detailed description of the expression patterns of this transgene in other body regions will be presented elsewhere. Expression in the head begins at 11 hpf and, for the first time, has allowed us to follow whole populations of cranial NC in the living embryo, from their premigratory origins at 14 hpf (Fig. 3A,B), and along their migratory pathways up to 20 hpf (Fig. 3C). Expression also persists in cartilage at 48 hpf (Fig. 3I). Time-lapsed, confocal movies of *sox10:egfp* expression between 14-20 hpf revealed that NC at midbrain levels migrates

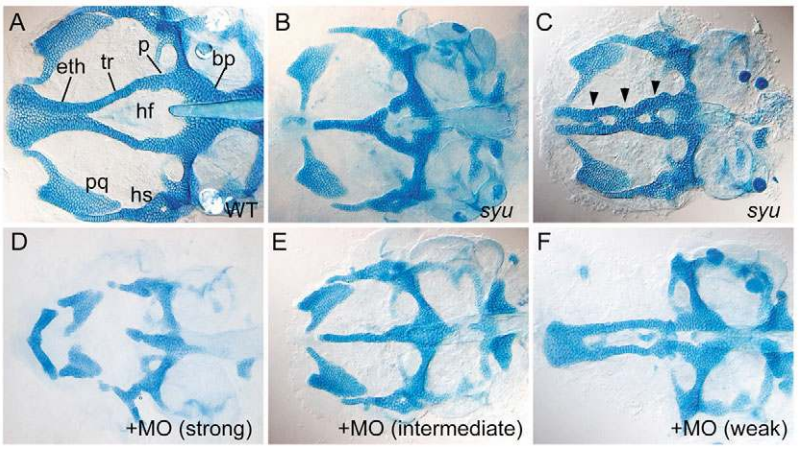

Fig. 1. Neurocranial cartilage patterns in wild-type and Hh-deficient larvae. Alcian stained cartilages were dissected and flat mounted; dorsal views are shown, anterior to the left. (A) The wild-type ANC at 4.5 dpf includes paired trabeculae (tr) and an ethmoid plate (eth). Mandibular (pq) and hyoid (hs) cartilages remain attached. (B,C) Neurocranial defects in *syu* mutants. Trabecular cartilages either fuse completely (B) or partially (C, arrowheads) at the midline. (D-F) Concentration-dependent effects of co-injected *shh*-MO and *twhh*-MO in wild type: (D) 3.0 ng *shh*-MO + 0.82 ng *twhh*-MO; (E) 2.0 ng *shh*-MO + 0.55 ng *twhh*-MO; (F) 1.0 ng *shh*-MO + 0.27 ng *twhh*-MO. bp, basal plate; eth, ethmoid plate; hf, hypophysial fenestra; hs, hyosymplectic; pq, palatoquadrate; p, polar cartilage; tr, trabeculae.

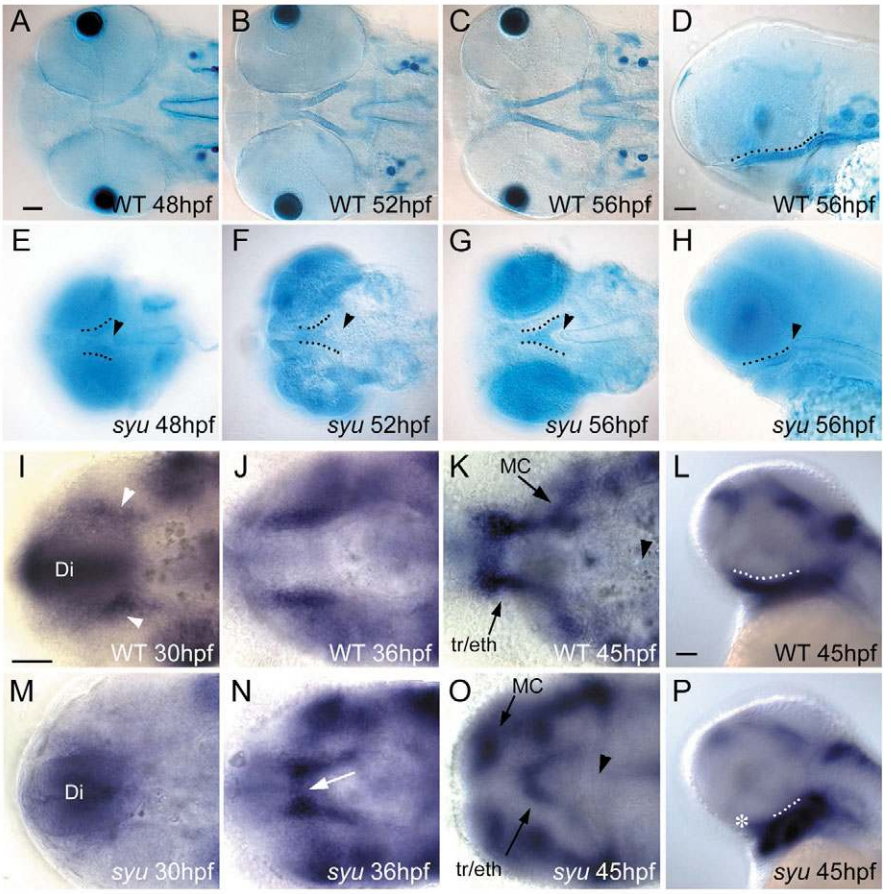

Fig. 2. Early chondrogenesis in the ANC. (A-H) Alcian Blue-stained embryos. (I-P) In situ hybridization for *sox9a* mRNA. Ventral views in wild type (A-C) and in *syu* mutants (E-G) between 48-56 hpf are shown. (A) Paired trabeculae consist of single rows of chondrocytes. (B,C) These elongate (B) and fuse posteriorly (C) to the parachordals. (D) Lateral view, 56 hpf, showing the ventral position of trabeculae (dotted line). (E) In *syu* mutants, the first ANC cartilages (dotted lines) are shorter and closer to the notochord (arrowhead). (F) Trabeculae fuse at the midline and (G) this fusion persists. (H) A lateral view of a *syu* mutant at 56 hpf. (I-K) Ventral views of *sox9a* expression in wild type between 30-45 hpf. (M-O) *sox9a* expression in *syu* mutants. (I) Early expression in bilateral cell clusters (arrowheads) adjacent to the diencephalon (Di). (J,K) These elongate posteriorly (J), and fuse in the midline anteriorly (K). (L) Lateral view of wild type at 45 hpf. (M) In *syu* mutants, *sox9a* expression is delayed. (N,O) *sox9a*+ clusters elongate (N) and fuse anteriorly (O, arrow). (P) Lateral view of *sox9a* expression in *syu* mutants showing fused trabeculae (dotted lines). Asterisk indicates anterior extent of expression. eth, ethmoid plate; MC, Meckel's cartilage; tr, trabeculae. Scale bar: 50 μm.

anteriorly, between the eyes, into the position of the future ANC (Fig. 3B,C; see Movie 1 in the supplementary material). Tracking of individual cells in these movies revealed a general tendency for NC cells originating in more anterior positions to migrate with more anterior trajectories (Fig. 3D). NC cells that originate at anterior midbrain levels, tend to move along the dorsal edge of the optic vesicle to the anterior tip of the embryo (n=4). By contrast, NC cells that originate further posteriorly, near the midbrain-hindbrain boundary, follow a more ventral trajectory posterior to the eyes by 20 hpf (n=8). Through these movements, NC eventually forms a continuous band of cells that surround the posterior and medial portions of the eyes, the future locations of cartilages of the ANC.

We also examined later stages of NC morphogenesis at the ventral midline in *sox10:egfp* transgenic embryos. In uninjected controls at 24 hpf, *sox10:egfp*+ cells from the hindbrain aggregate in the pharyngeal arches, whereas others are widely distributed around the brain and eyes (Fig. 3E). Precursors of the trabeculae at this stage lie beneath the eye, anterior to the stomodeum (arrowhead in Fig. 3E) that delineates the mandibular arch (PA1). These cells are widely separated (~100 μm) from one another across the midline at 24 hpf, on either side of the brain and pharynx (Fig. 3F,G). *sox10:egfp*+ cells in this region first aggregate around the mouth at 36 hpf (Fig. 3H), and condense to prefigure trabeculae by 42 hpf (data not shown), six hours prior to cartilage differentiation (Fig. 3I). Once cartilage has differentiated, sox10:egfp expression also includes other cartilages such as the parachordals and the pectoral girdle, which derive from embryonic mesoderm (data not shown).

Next, we investigated NC migration in Hh-deficient embryos using *sox10:egfp*. This revealed little difference from controls at early stages (n=3, data not shown). At 24 hpf, the head is slightly reduced but the pattern of *egfp*+ NC cells is similar to controls when viewed laterally (Fig. 3J). A ventral view, however, reveals a dramatic difference. NC cells lying anterior to the mandibular arch fuse across the ventral midline, between the eyes (Fig. 3K,L). Fusion is more pronounced at 36 hpf (Fig. 3M), and leads directly to a midline condensation that forms a single rod of cartilage (Fig. 3N). This midline structure is most likely a fusion of trabeculae, based on the relative positions of the adjacent palatoquadrate and the anterior end of the notochord in Hh-deficient embryos. These defects in Hh-deficient embryos do not appear to result from elevated NC cell death, as determined by acridine orange staining (data not shown). Taken together, these results suggest that Hh signaling is required for the morphogenetic movements that separate NC streams at the ventral midline.

Separate origins for trabecular and medial ethmoid cartilages in the NC

To confirm cartilage identities in *syu* mutants, we labeled individual premigratory NC cells with fluorescent lineage tracers and tracked their fates in the ANC at 80-85 hpf. In the initial experiments, the lipophilic fluorescent dye, PKH26, was injected extracellularly at different positions in the NC of *sox10:egfp* transgenics at 13 hpf and followed until they

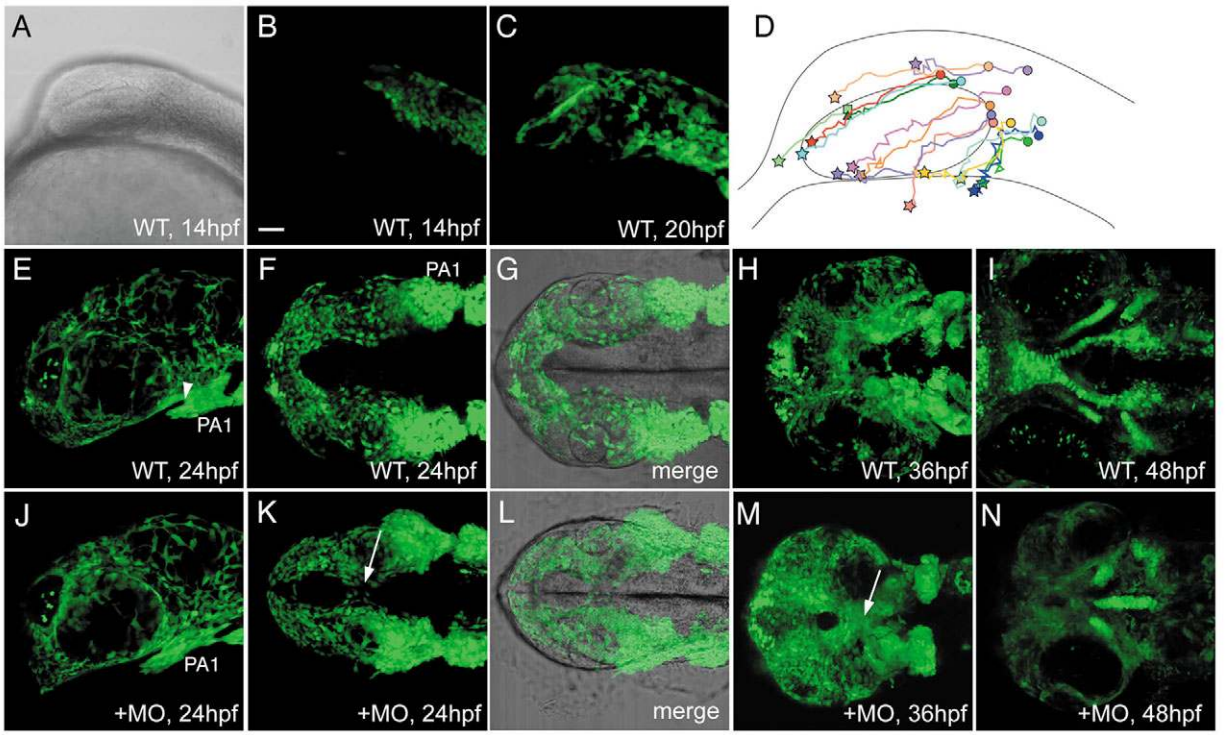

Fig. 3. Expression of the *sox10:egfp* transgene in cranial NC cells of living embryos. (A-C) Representative images from a confocal, time-lapsed movie of *sox10:egfp* expression in the head between 14-20 hpf, lateral view (see also Movie 1 in the supplementary material). (A-C) Brightfield (A) and confocal images (B,C) at 14 hpf (A,B) and 20 hpf (C). (D) Diagram illustrating migration paths of individual NC cells, traced by analyzing confocal stacks within the movie. Circles indicate premigratory cell positions and stars indicate their positions six hours later. Some cells (dark green triangle) could not be tracked beyond 17.5 hpf, whereas others (light green square) were only traceable after 16.5 hpf. (E-N) *sox10:egfp*+ cells at later stages in wild-type (E-I) and Hh-deficient (J-N) embryos. (E) Lateral view at 24 hpf, showing the first pharyngeal arch (PA1) and stomodeum (arrowhead). Precursors of the ANC lie beneath the eye and anterior to this stomodeal pouch. (F,G) Ventral views with (G) and without (F) accompanying brightfield images. (H,I) By 36 hpf, *sox10:egfp*+ cells aggregate around the mouth (H), and, by 48 hpf, form cartilage of the ANC (I). (J) In Hh-deficient embryos, *sox10:egfp* expression is similar to that seen in wild-type controls, when viewed laterally. (K,L) However, in ventral view the head is mediolaterally compressed, and NC cells anterior to PA1 fuse across the ventral midline, between the eyes (arrow). (M) Fusion is more pronounced at 36 hpf, forming a single midline condensation (arrow). (N) A single rod of *sox10:egfp*+ cartilage forms in the midline by 48 hpf. Scale bar: 50 μm.

formed cartilage (Fig. 4). This technique typically labeled 5-10 cells. When NC were labeled at the anterior midbrain, just dorsal to the eye (Fig. 4A,K; 200-300 μm from the anterior end), cells were later found in the medial ethmoid, confined to a triangular group of chondrocytes wedged between the anterior ends of the trabeculae (Fig. 4B; *n*=15). By contrast, cells labeled further posteriorly, by the midbrain-hindbrain boundary (Fig. 4E,K; 300-400 μm) generated progeny confined to the trabecular rods and lateral ethmoid, but not in the medial ethmoid (Fig. 4F; *n*=15). We confirmed these results by labeling single NC cells intracellularly with iontophoresis of fluorescent dextrans in *sox10:egfp* transgenics (see Fig. S1 in the supplementary material). Our fate map for the ANC roughly coincides with the anterior limits of *sox10* and *foxd3* expression in NC (Fig. 4I,J). These domains are changing rapidly, as one hour earlier (12 hpf) we could not distinguish the positions of ethmoid and trabecular precursors.

To further investigate the distinct origins of these two skeletal regions, we also made a fate map at 22-24 hpf, near the end of NC migration. Postmigratory NC cells were labeled with PKH26 at three different locations: (1) the anterior end of the head; (2) ventral-anterior to the eye; and (3) ventral-posterior to the eye. When cells at the anterior end were labeled, their progeny formed the median ethmoid plate (Fig. 4C,D; *n*=8). By contrast, cells ventral-anterior or ventral-posterior to the eye formed lateral ethmoid and trabecular cartilage (Fig. 4G,H; Fig. S2 in the supplementary material; *n*=15). Similar results were obtained by iontophoretically labeling single NC cells (see Fig. S2 in the supplementary material). These results confirm that NC cells that form the median ethmoid are distinct and follow different migratory pathways, rather than forming as medial trabecular expansions (Fig. 4K).

To confirm the identity of the single midline cartilage in Hh-deficient animals, we performed similar fate mapping studies (Fig. 5A,C). Although posterior cells that normally form the trabeculae and lateral ethmoid contributed to the midline cartilage rod in Hh-deficient animals (Fig. 5D; *n*=5), more anterior NC cells that normally form the medial ethmoid did not form cartilage (Fig. 5B; *n*=5). Some labeled, undifferentiated cells were found in the tissue surrounding the cartilage, suggesting that medial ethmoid progenitors were eliminated in these embryos. Thus, the midline cartilage in Hh-deficient animals arises from the same NC population as trabecular precursors in wild type do.

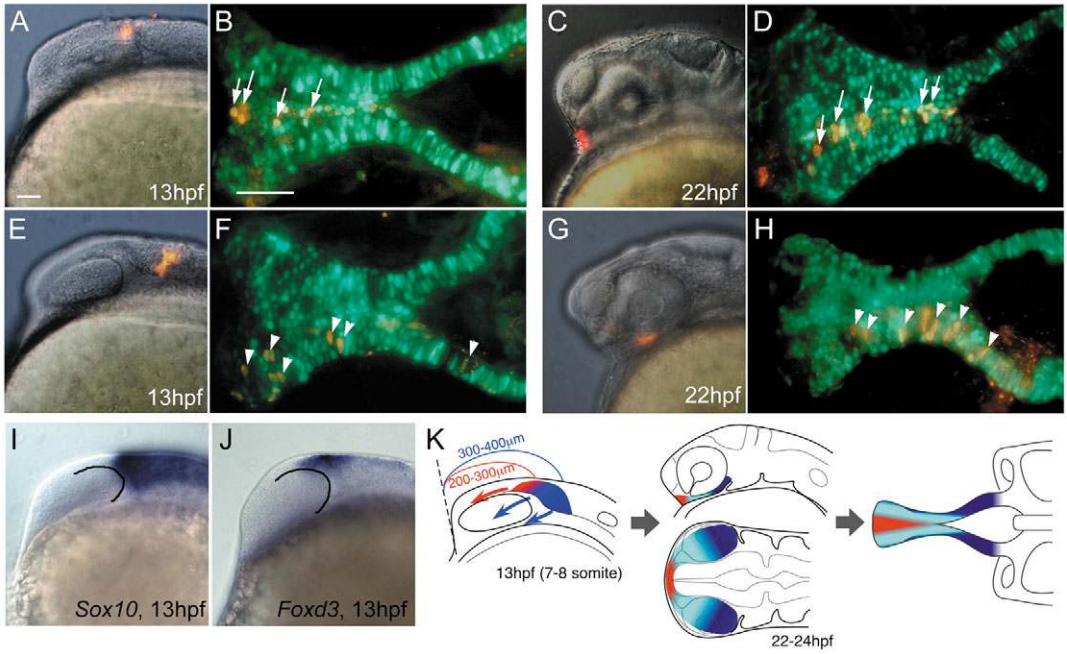

Fig. 4. Fate maps of NC contributions to the ANC. (A,C,E,G) Labeled cells immediately after injection of PKH26, seen in lateral views of living embryos at 13 hpf. (B,D,F,H) Labeled cartilage in the ANC at 80-85 hpf, showing co-localization (yellow) of PKH (red) and *sox10:egfp* (green), ventral view. (A) Premigratory cranial NC dorsal to the optic vesicle forms median ethmoid (B, arrows). (E) Premigratory NC posterior to the optic vesicle forms trabeculae (F, arrowheads). (C) Postmigratory NC cells anterior to the optic stalk at 22-24 hpf form median ethmoid (D, arrows). (G) Postmigratory NC posterior to the optic stalk form trabeculae (H, arrowheads). (I,J) Expression of *sox10* (I) and *foxd3* (J) mRNA at 13 hpf, lateral view. Lines delineate the posterior edge of the optic vesicle. (K) Schematic representation of the fate map. In premigratory NC, ethmoid precursors (red) migrate anteriorly, trabecular precursors (blue) migrate laterally and ventrally. Scale bars: 50 μm; in A for A,C,E,G,I,J; in B for B,D,F,H.

Separate early and late requirements for Hh signaling

To determine the precise temporal requirements for Hh signaling in the ANC, we blocked Hh signaling using the plant-derived steroidal alkaloid cyclopamine (CyA). CyA directly antagonizes the Hh signal-activation component Smoothened (Cooper et al., 1998; Chen et al., 2002). Embryos were bathed in CyA at different stages between 0-48 hpf and stained for cartilage. Siblings treated in parallel were stained by in situ hybridization for *patched 1* (*ptc1*) at 24-36 hpf as a control for loss of Hh activity in NC (data not shown). Embryos treated with low concentrations (5 μM) for a 4-hour period during gastrulation between 4-8 hpf had trabecular fusions similar to *syu* mutants (Fig. 6B,C; *n*=30; 50%), and, at these concentrations, *ptc1* expression was reduced but not eliminated in the NC (data not shown). Higher concentrations, 50-100 μM, applied over a similar time period, effectively blocked all *ptc1* expression and prevented all cartilage formation anterior to the basicapsular commissure (Fig. 6D). We were surprised at first to find that treatments with these high concentrations for any 4-hour period between 0-24 hpf caused a complete loss of the ANC (Fig. 6E), indicating an absolute requirement for Hh signaling in ANC development during NC migration. However, even early treatments suppress *ptc1* expression up to at least 36 hpf, indicating that suppression of Hh signaling by CyA persists long after its removal.

Surprisingly, 50 μM CyA treatment of older embryos (>24 hpf), after NC migration, still disrupted trabecular and ethmoid development. Treatment between 24-30 hpf eliminated most of

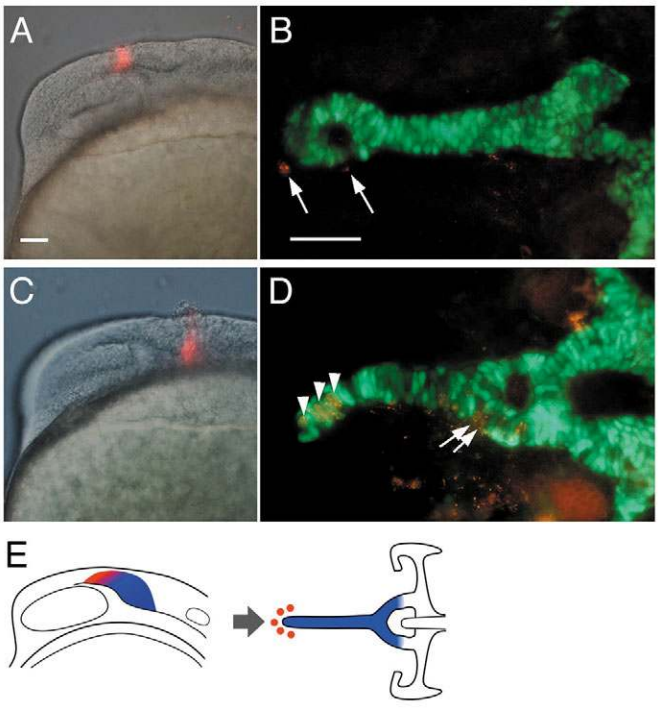

Fig. 5. Fate maps in Hh-deficient embryos. (A,C) PKH labeling immediately after injection, lateral views. (B, D) Labeled cells at 80 hpf derived from these injections, showing co-localization (yellow) of PKH (red) and *sox10:egfp* (green) in dissected preparations, ventral views. (A) NC cells labeled dorsal to the optic vesicle do not contribute to cartilage, but remain undifferentiated (B, arrows). (C) By contrast, cells labeled posterior to the optic vesicle contribute to the midline cartilage rod (D, arrowheads) and posterior trabeculae (arrows). (E) Schematic representation of the fate map in Hh-deficient embryos. Trabecular precursors form cartilage (blue), whereas ethmoid progenitors (red) do not. Scale bars: 50μm; in A for A,C; in B for B,D.

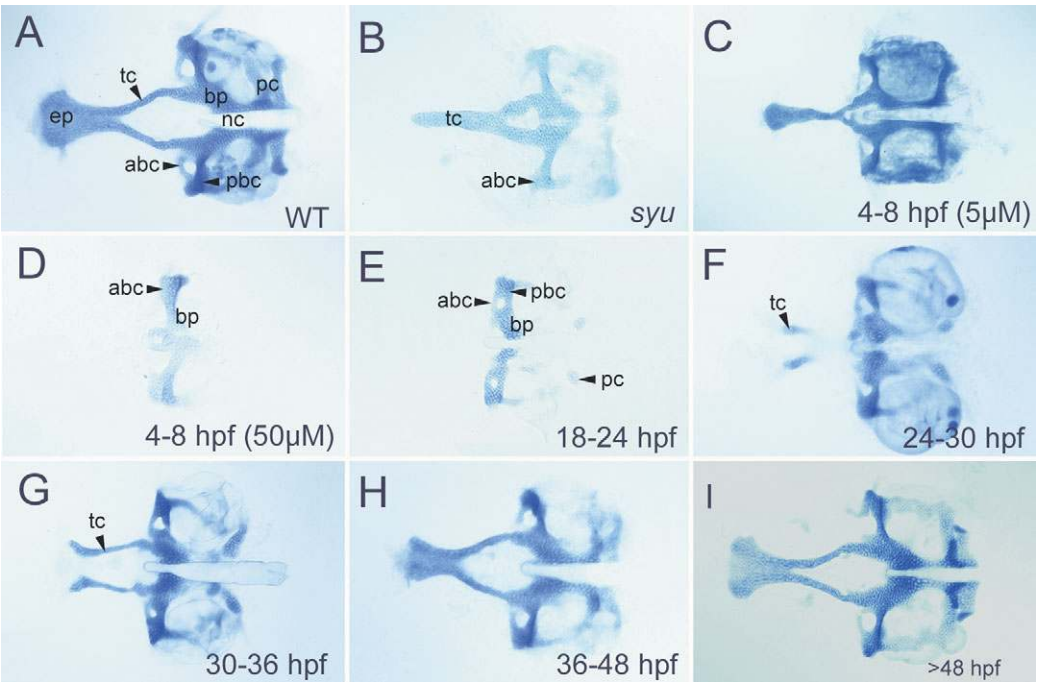

Fig. 6. CyA treatment disrupts ANC formation. Flat-mounted, Alcian Blue stained cartilages at 5 dpf; anterior is to the left. (A) Wild type. (B) *syu* mutant. (C) A wild-type treated with 5 μM CyA from 4-8 hpf. (D-I) Wild-type larvae treated with 50 μM CyA at different stages between 18-60 hpf. (D,E) Treatment between 4-24 hpf eliminates all ANC cartilage. (F) Treatment between 24-30 hpf eliminates most cartilage, although some trabecular cartilage forms but never fuses to the posterior neurocranium. (G) Treatments between 30-36 hpf eliminate the ethmoid, but not trabeculae. (H,I) Treatments later than 40 hpf cause slight reductions in the ANC. abc, anterior basicapsular commissure; bp, basal plate; ep, ethmoid plate; nc, notochord; pbc, posterior basicapsular commissure; pc, parachordal cartilage; tc, trabeculae.

the ANC, other than a few trabecular chondrocytes, in the location where these cartilages first differentiate in wild types (Fig. 6F; *n*=30; 90%). Treatment between 30-35 hpf eliminated the medial ethmoid plate, whereas trabecular cartilages were well formed, thereby creating a large palatal cleft (Fig. 6G). Embryos treated between 36-48 hpf showed slight reductions in the ANC (Fig. 6H). No defects were observed with treatments after 48 hpf (Fig. 6I).

Exogenous Shh causes midfacial expansion and promotes chondrogenesis

Next, we investigated the effects of increasing Hh signaling on ANC formation. We first injected mRNA for zebrafish *shh* to misexpress it throughout the embryo; this mRNA is only likely to persist through gastrula and neurula stages. The ANC of mRNA-injected wild-type embryos was roughly normal in shape but expanded laterally (Fig. 7B), and in some injected embryos, the medial and lateral ethmoid were separated (Fig. 7B), further suggesting that their precursors differentiate separately. To investigate later roles for Shh, after NC migration, we implanted Shh-coated beads and analyzed skeletal pattern in the ANC. Bead implantation at 20 hpf into the space between eye and brain in wild-type embryos promoted chondrogenesis in the ANC. Both ethmoid and trabeculae expanded laterally compared with BSA-soaked control beads. In some cases, posterior trabecular cartilages were fused to the dorsal (palatoquadrate) cartilage of the mandibular arch (Fig. 7C, compare with Fig. 1A).

Because *syu* mutants lack a functional Shh protein, we also tested whether Shh-coated beads could rescue *syu* or *shh/twhh*-MO injected embryos at different stages of ANC development. Implantation of a BSA-soaked control bead had no effect at any stage (Fig. 7D). By contrast, beads soaked in 10 μg/ml Shh implanted as late as 22 hpf partially restored both head size and ANC patterning in *syu* (Fig. 7E; *n*=15). Surprisingly, despite bead placement between the eye and midbrain on one side of the head, rescue often occured bilaterally to nearly a wild-type configuration. Others showed cartilage distortions or ectopic chondrocytes along the medial trabeculae (data not shown; *n*=10). To determine whether the postmigratory NC distribution is restored by these late Shh applications, we analyzed ANC precursors in MO-injected *sox10:egfp* embryos after bead implantation. With BSA-beads, *egfp*+ cells were observed in the midline at 36 hpf (Fig. 7G), showing that the beads themselves did not physically disrupt NC distribution. By contrast, when a Shh-coated bead was implanted at 22 hpf, separation was restored between groups of *sox10:egfp*+ cells on either side of the midline in *syu* mutants, although a few cells remained at the midline in some cases (Fig. 7H). Overall head size was not rescued in these experiments (compare Fig. 7G and H with I), suggesting that the role of Hh signaling in midline separation of NC is not simply in growth. These results show that exogenous Hh can rescue ANC pattern in Hh-deficient zebrafish embryos by restoring the cranial NC distribution. They also suggest that the pre-chondrogenic pattern in the ANC is not specified at 22 hpf. By 30 hpf, Shh-coated beads can only partially rescue the *syu* phenotype (Fig. 7F), and a few hours later they have no effect.

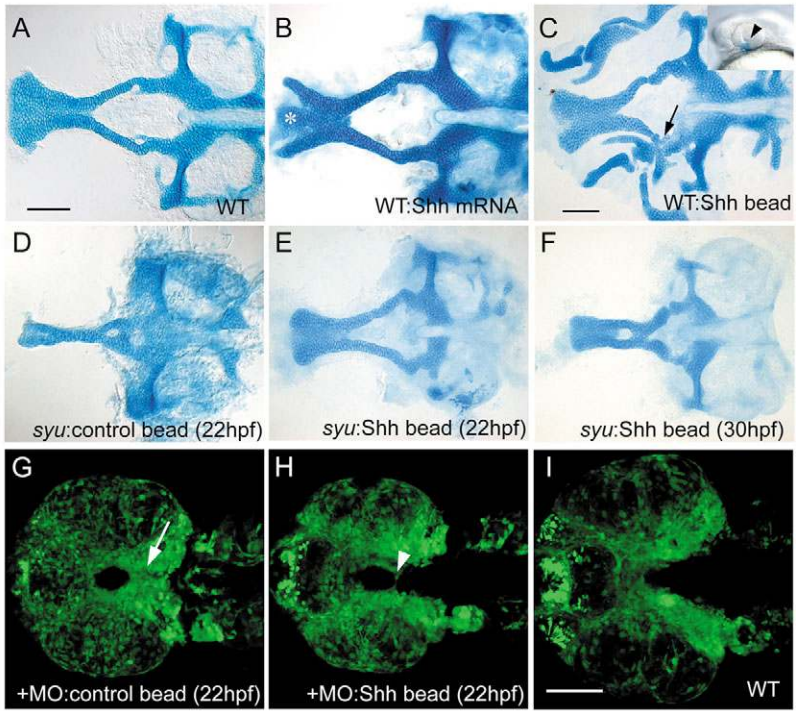

Fig. 7. Exogenous Shh expands ANC cartilage in wild types and rescues *syu* mutants. Ventral views, anterior to the left. (A-F) Flat-mounted, Alcian-Blue-stained cartilages at 4.5 dpf. (G-I) Confocal images of *sox10:egfp* expression in dissected embryos at 36 hpf. (A) Wild type. (B) Wild type injected with *shh* mRNA. Trabeculae expand laterally and often separate from the ethmoid (asterisk). (C) Wild type implanted with a Shh-coated bead on the left side at 20 hpf. The ANC expands near the bead; both trabeculae and ethmoid thicken, and the trabecula on the implanted side fuses to the palatoquadrate (arrow). Inset shows the typical bead position (arrowhead). (D) Control beads implanted at 22 hpf had no effect on ANC formation in *syu* mutants. (E) Implantation of a Shh-coated bead partially rescues the ANC in *syu* mutants. (F) Bead implantation at 30-36 hpf also partially rescues the ANC in some cases. (G) Control beads implanted between 22-36 hpf had no effect on the distribution of *sox10:egfp*+ cells in Hh-deficient embryos. Arrow indicates NC cells at the midline. (H) Implantation of a Shh-coated bead at 22 hpf rescued *sox10:egfp* expression at the ventral midline (arrowhead). Note that the width of the bead-implanted embryos is identical to that of controls (G,H), and smaller than that of wild type (I). Scale bars: 50 μm; in A for A,B; in C for C-F; in I for G-I.

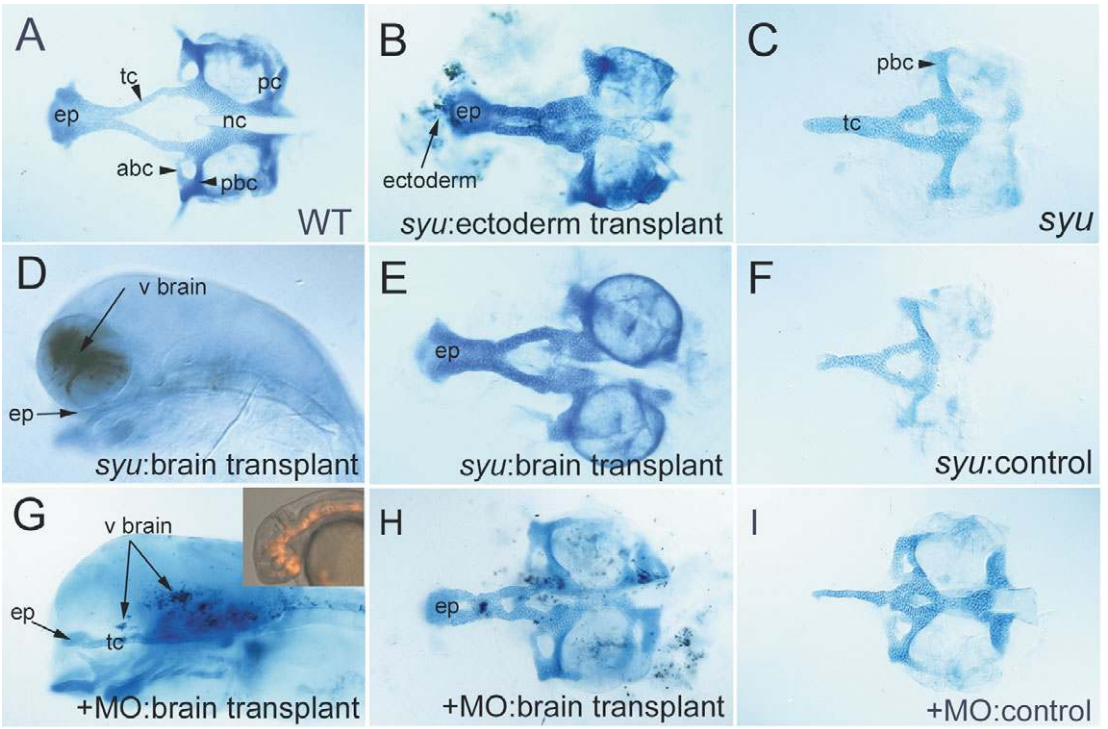

Fig. 8. Shh is required in both ventral neural tube and oral ectoderm for ANC formation. (A-C,E,F,H,I) Flat-mounted Alcian-Blue stained cartilage at 5 dpf; anterior is to the left. (D,G) Lateral views of transplants shown in E and H, prior to cartilage dissection. Transplanted donor cells (brown) lie in the ventral brain. (A) Wild type. (B) Partial rescue of the ANC by wild-type ectoderm transplanted into a *syu* mutant host. Transplanted cells lie close to the ethmoid plate in this example. (C) *syu* control sibling of the embryo shown in B. (D) Grafted wild-type cells in the ventral forebrain of a *syu* mutant. (E) Partial rescue of the ANC by the transplant shown in D. Grafted cells were lost during dissection. (F) *syu* control sibling of embryo shown in E. (G) An *shh*-MO/*twhh*-MO-injected embryo. Inset shows transplanted cells at 28 hpf. (H) Partial rescue of ANC in the embryo shown in G. (I) *shh*-MO/*twhh*-MO-injected control sibling of embryo in H. abc, anterior basicapsular commissure; ep, ethmoid plate; nc, notochord; pbc, posterior basicapsular commissure; pc, parachordal cartilage; tc, trabeculae.

Distinct Shh sources in the floorplate and oral ectoderm induce the ANC

Shh is a secreted protein expressed in several different cranial tissues in the embryo, including the ventral brain, facial ectoderm and pharyngeal endoderm. To address which is required for ANC development, we used mosaic analysis to test the capacity of wild-type cells to rescue ANC development when transplanted into Hh-deficient hosts. Surface ectodermal cells that form epidermis arise from ectoderm near the animal pole of the early gastrula at 6 hpf (Kimmel et al., 1990). Cells were grafted from this location in a wild-type donor embryo co-injected with fluorescent lineage tracers, into the same region in *syu* mutants and raised to 96 hpf for cartilage staining. These ectodermal grafts expressed *shh* mRNA (data not shown) and partially rescued trabecular and ethmoid chondrogenesis (Fig. 8A-C; *n*=3). Rescue only occurred when transplanted cells were located in dorsal oral ectoderm, just above the mouth, that comes to lie beneath the ethmoid (Fig. 8B). To target cells to the ventral forebrain, similar transplants were performed with ectoderm from the dorsal side of the early gastrula near the margin at 6 hpf, where these cells share a common lineage with floorplate cells at posterior hindbrain and spinal levels (Hatta et al., 1991). Dye-labeled cells were grafted from this location in wild type into the same region of *syu* or *shh/twhh*-MO injected hosts, and stained for cartilage (Fig. 8D-I). In some cases, these transplants also rescued bilateral trabecular separation (Fig. 8E; *n*=5).

Shh may act directly on NC or through intermediate signals, but recent tissue-specific removal of *Smo* function from NC in mice suggests that it acts directly on skeletal progenitors. To distinguish between these hypotheses, we transplanted labeled NC cells from *smu* mutants, which lack a functional Smo, into the wild-type midbrain NC and followed their fates at 96 hpf (Schilling and Kimmel, 1994) (see also Fig. S3 in the supplementary material). These transplanted cells migrated with the host NC but remained undifferentiated and never formed cartilage (0%, *n*=6). Controls in which wild-type cranial NC cells were transplanted similarly formed cartilage in the ANC at a high frequency (data not shown; 60%, *n*=25). These results demonstrate that *smu* is required cell autonomously for skeletogenesis in cranial NC, and suggests that Hh acts directly on NC to induce the ANC.

Discussion

The anteriormost NC cells in all vertebrate embryos migrate between the eyes to form the anterior neurocranium (ANC) and palate, as well as part of the lower jaw (Stone, 1929; Kontges and Lumsden, 1996). Here, we show that, in zebrafish, the two main cartilages of the larval ANC, the ethmoid plate and trabeculae, arise from distinct precursors (Fig. 9A), and both depend on Hh signaling for their development. In humans, loss-of-function mutations in the *SHH* gene cause holoprosencephaly (HPE) accompanied by facial anomalies including cyclopia, a single nostril, and cleft lip or palate (Gorlin et al., 1990; Roessler et al., 1996; Nanni et al., 1999). Similarly, disruption of Hh signaling in *syu* mutant zebrafish or in embryos treated with CyA during gastrulation causes cyclopia, and this is associated with trabecular fusions and loss of the median ethmoid. Genetic screens in the zebrafish have identified many loci required for ML patterning of the larval

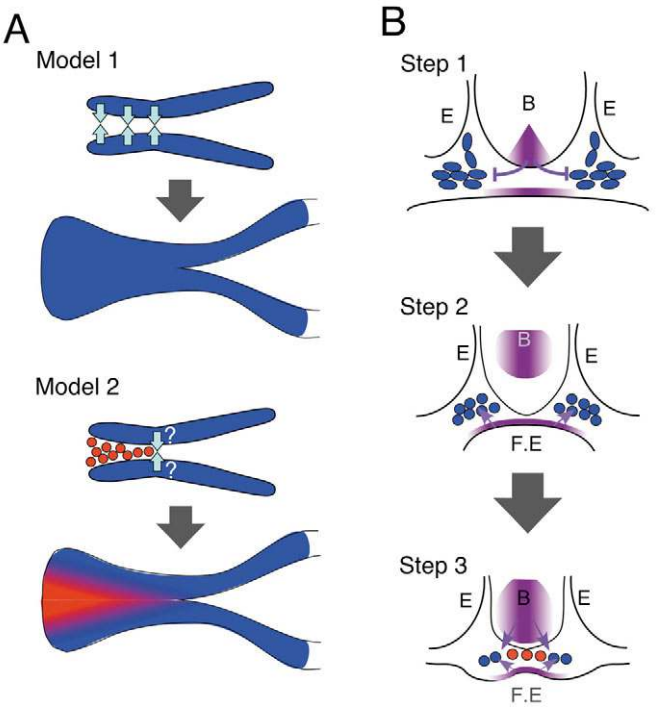

Fig. 9. Models for the role of Hh signaling in ANC development. (A) Diagrams illustrate trabecular cartilage (blue). (Model 1) Classical model: trabecular rods fuse anteriorly to form the trabeculae communis and ethmoid plate (arrows). (Model 2) New model: separate origins for the medial ethmoid (red) and trabeculae (except a small trabeculae communis, arrows). (B) Diagrams of transverse sections illustrate three proposed steps by which Shh controls ANC patterning and chondrogenesis. (Step 1) Shh from ventral neuroectoderm (purple) prevents mixing of migrating NC cells (blue ovals) at the midline. (Step 2) Shh from facial ectoderm (F.E.) promotes trabecular chondrogenesis (arrows). At this stage, *shh* expression in the CNS does not extend into the ventral hypothalamus, and is therefore unlikely to influence the ANC. (Step 3) Ethmoid precursors (red and blue circles) are induced to chondrify by Hh secreted from both the ventral hypothalamus, and the facial ectoderm (F.E).

ANC, some of which encode Hh signaling components (Brand et al., 1996; Schuarte et al., 1998; Karlstrom et al., 1999). We show that fusions result from aberrant NC cell mixing at the ventral midline, and a lack of chondrogenesis in the ANC. Our cell transplantation studies suggest that there are two important Shh sources in this process, the ventral neural tube and the oral ectoderm, consistent with previous studies in chick (Hu et al., 2003). We propose that Hh signaling is required at two separate stages in the ANC: one early that acts to separate cells at the midline, and a second, more prolonged period in which it promotes chondrogenesis (Fig. 9B). We argue that this helps to explain the spectrum of phenotypes that have been described for Hh deficiencies in fish, chick and mouse, as well as the facial defects associated with human HPE.

Distinct origins of medial and lateral neurocranial cartilage

Cranial NC cells from the midbrain that form the larval ANC do not all follow the same migratory path. The path choice depends on their premigratory locations at anterior or posterior

midbrain (Fig. 3). We traced living NC cells in *sox10:egfp* transgenic embryos and found that cells from the anterior midbrain migrated along the dorsal optic vesicle and optic stalk. By contrast, NC cells from the posterior midbrain migrated behind the optic stalk, many accumulating posterior to the optic vesicle, in a 'premandibular' location. These results confirm previous fate maps (Lumsden et al., 1991; Ohsumi-Yamashita et al., 1994; Epperlein et al., 2000) but, until now, the migratory pathways of these cells have only been inferred.

We also show that the AP position of a premigratory NC cell beside the midbrain predicts its fate in the skull (Fig. 4K). By following clones of single cells or small groups labeled with fluorescent lineage tracer dyes, we confirmed that cells migrating along the more anterior pathway above the eye exclusively form median ethmoid cartilage, whereas cells migrating along the more posterior path behind the eye form the trabeculae. Our results corroborate previous fish, amphibian and avian fate maps, showing that the trabeculae cranii derive from mesencephalic NC (Landacre, 1921; Stone, 1929; Langille and Hall, 1988) but reveal an additional, more anterior, ethmoid progenitor population. Thus, rather than simply arising as a medial growth and fusion of the trabeculae (trabeculae communis; Fig. 9A, top panels), as previously assumed (De Beer, 1937; Bertmar, 1959), the medial ethmoid and perhaps other midline skeletal elements have a distinct cellular origin (Fig. 9A, bottom panels), possibly under distinct genetic control. In support of this hypothesis, in *schmalspur* (*sur*) mutant zebrafish, trabecular defects occur without corresponding changes in the ethmoid plate (Brand et al., 1996), whereas other mutants show defects restricted to the ethmoid (Neuhauss et al., 1996; Piotrowski et al., 1996). More long-term fate mapping studies are required to determine whether nasal and palatal progenitors, which differentiate between 1 and 3 weeks postfertilization in zebrafish (Cubbage and Mabee, 1996), also arise from this anterior NC. These results also have important implications for the interpretation of gene expression patterns in the premigratory NC, which in some cases do not include the most anterior, ethmoid domain.

We also labeled NC cells later, during migration, and followed the contributions of cells along each pathway to cartilage in the ANC. Consistent with our fate maps at earlier stages, we found that only cells at the anterior end near the midline contributed to the medial ethmoid plate. The trabeculae are formed by NC cells that lie more posteriorly, many developing in close association with the mandibular arch. Several recent papers have highlighted similar cells in amphibian and avian embryos, and have argued that they are a part of the mandibular arch, blurring the distinction between maxillary and mandibular (Cerny et al., 2004). Our results indicate that a majority of these cells lie anterior to the stomodeum in zebrafish, just outside of the mandibular arch. In other respects, our fate map is similar to those for the facial prominences in other species (McGonnell et al., 1998).

Hh signaling at the midline is required for both NC morphogenesis and chondrogenesis

The variety of skeletal defects caused by Hh-deficiencies remains unexplained. For example, within the spectrum of human patients with Hh-associated HPE, some show midline collapse of facial structures, while others show clefting (Roessler and Muenke, 2001; Roessler and Muenke, 2003). Our studies suggest that such phenotypic differences reflect stage-dependent requirements for Hh signaling; and separate roles in midline separation and chondrogenesis. We have shown that early NC migration is unaffected in Hh-deficient embryos and that Hh acts later to prevent NC cells from crossing the midline. Shh may induce midline tissue expansion that acts as a physical barrier to movement (Fig. 9B, Step 1). Shh has anti-apoptotic activity (Charrier et al., 2001), and also promotes cell survival and growth in the ventral brain (Britto et al., 2002). Our analysis of *sox10:egfp* suggests that this is not simply an affect on growth, although we have not formally ruled out this possibility. We did not observe elevated NC apoptosis in Hh-deficient embryos (data not shown), which is consistent with previous reports (Cordero et al., 2004). Alternatively, Shh may directly alter NC cell movements in a concentration-dependent manner, as it has been shown to modify adhesion and NC migration in vitro (Testaz et al., 2001), or may act indirectly to induce a second signal from midline tissue(s), that acts on NC. At least some of these requirements for Hh signaling are direct, as NC cells transplanted from *smo* mutants into wild-type hosts never form cartilage (see Fig. S3 in the supplementary material), similar to recent findings in mice with a tissue-specific loss of *Smo* function in NC (Jeong et al., 2004). Future studies are needed to dissect how these early patterning influences of Hh on NC morphogenesis are coupled with effects on growth.

Two lines of evidence point to the fact that there are separate early and late roles for Hh-signaling in skull development (Fig. 9B, Step 2 and Step 3). First, CyA treatment between 24-36 hpf disrupts ANC chondrogenesis, but no longer affects NC morphogenesis at the midline. Similarly, a lack of Hh-signaling in *Shh*- or *Smo*-mutant mice causes severe cranial bone loss, and in some cases palatal clefting, presumably when ethmoidal chondrogenesis is disrupted. Late CyA treatment causes similar clefts in chick, suggesting that this late requirement is conserved (Cordero et al., 2004). Our results are also consistent with numerous studies in mammals implicating Hh proteins in skeletal differentiation (reviewed by Karsenty and Wagner, 2002; Kronenberg, 2003; Zelzer and Olsen, 2003). In our model, if there is sufficient signaling to separate NC at the midline, but not for ethmoid induction, clefting may result.

Multiple Hh sources induce neurocranial chondrogenesis

Not all forms of HPE in humans are accompanied by midline facial defects, suggesting that skeletal defects are not simply secondary consequences of forebrain defects. Our mosaic analyses help to explain this, and suggest that ectodermal Hh sources are also crucial for ANC formation. Gastrulation is the only period when CyA treatment in zebrafish causes midfacial fusions, and at these stages our data suggest that the important Hh source is the neural tube. Wild-type ventral neural tube cells locally rescue ANC development when grafted into the forebrain in Hh-deficient embryos, and separate the trabeculae at the midline. However, oral ectodermal grafts can also rescue chondrogenesis in the ANC (Fig. 8). These results are consistent with studies in chick suggesting that Shh from the facial ectoderm promotes maxillary and frontonasal outgrowth (Hu and Helms, 1999; Hu et al., 2003; MacDonald et al., 2004). Ectodermal sources may act together with Shh from the ventral

diencephalon and presumptive hypothalamus at these later stages to regulate chondrogenesis.

Taken together, our results suggest that the mechanisms by which Shh controls the coordinated growth and fusion of facial primordia are highly conserved among vertebrates. The ventral neural tube and oral ectoderm at the midline appear to form an organizing center controlling skeletal growth and morphogenesis. These tissues both express *shh*, and we argue that skeletogenic NC cells must interpret their positions relative to these midline sources of *shh* and differentiate accordingly. Interestingly, mutations in mice and humans that disrupt squamous epithelia also often cause cleft lip and palate (EEC syndrome), presumably reflecting defects in these epithelial signaling centers (Celli et al., 1999). An interesting direction for the future would be to explore the roles of other growth factors in the cranial ectoderm, and their interactions with Shh in skeletogenesis. As a starting point, mutagenesis screens in zebrafish have uncovered large phenotypic classes of mutants that disrupt the midline, many of which disrupt signaling by the TGFβ family member Nodal (Kimmel et al., 2001). Zebrafish Nodal-related proteins were recently shown to directly regulate *shh* expression in the zebrafish midline (Muller et al., 2000) and recent evidence in humans has implicated defects in Nodal signaling in HPE (Gripp et al., 2000). With the large mutant collection in zebrafish, we can now begin to study of how such pathways interact during palatal development.

We thank J. Eberhard and C. Kimmel for sharing information prior to publication. We also thank I. Blitz and Schilling Laboratory members for discussions and comments on the manuscript. This work was supported by grants from the March of Dimes (1-FY01-198), NIH (NS-41353, DE-13828) and Pew Scholars Foundation (2615SC) to T.F.S., Wellcome Trust to R.N.K., and an ORS award to T.J.C.

Supplementary material

Supplementary material for this article is available at
http://dev.biologists.org/cgi/content/full/132/17/3977/DC1

References

Ahlgren, S. C., Thakur, V. and Bronner-Fraser, M. (2002). Sonic hedgehog rescues cranial neural crest from cell death induced by ethanol exposure. *Proc. Natl. Acad. Sci. USA* **99**, 10476-10481.

Bertmar, G. (1959). On the ontogeny of the chondral skull in Characidae, with a discussion on the chondrocranial base and the visceral chondrocranium in fishes. *Acta Zool.* **40**, 203-364.

Brand, M., Heisenberg, C.-P., Warga, R. M., Pelegri, F., Karlstrom, R. O., Beuchle, D., Picker, A., Jiang, Y.-J., Furutani-Seiki, M., VanEeden, F. J. M. et al. (1996). Mutations affecting development of the midline and general body shape during zebrafish embryogenesis. *Development* **123**, 129-142.

Britto, J., Tannahill, D. and Keynes, R. (2002). A critical role for sonic hedgehog signaling in the early expansion of the developing brain. *Nat. Neurosci.* **2**, 103-110.

Celli, J., Duijf, P., Hamel, B. C., Bamshad, M., Kramer, B., Smits, A. P., Newbury-Ecob, R., Hennekam, R. C., Van Buggenhout, G., van Haeringen, A., et al. (1999). Heterozygous germline mutations in the p53 homolog p63 are the cause of EEC syndrome. *Cell* **99**, 143-153.

Cerny, R., Lwigale, P., Ericsson, R., Meulemans, D., Epperlein, H.-E. and Bronner-Fraser, M. (2004). Developmental origins and evolution of jaws: new interpretation of "maxillary" and "mandibular". *Dev. Biol.* **276**, 225-236.

Charrier, J.-B., Lapointe, F., Le Douarin, N. M. and Teillet, M.-A. (2001). Anti-apoptotic role of Sonic hedgehog protein at the early stages of nervous system organogenesis. *Development* **128**, 4011-4020.

Chen, J. K., Taipale, J., Cooper, M. K. and Beachy, P. A. (2002). Inhibition of hedgehog signaling by direct binding of cyclopamine to smoothened. *Genes Dev.* **16**, 2743-2748.

Chen, W., Burgess, S. and Hopkins, N. (2001). Analysis of zebrafish smoothened mutant reveals conserved and divergent functions of hedgehog activity. *Development* **128**, 2385-2396.

Chiang, C., Litingtung, Y., Lee, E., Young, K. E., Corden, J. L., Westphal, H. and Beachy, P. A. (1996). Cyclopia and defective axial patterning in mice lacking Sonic hedgehog gene function. *Nature* **383**, 407-413.

Chibon, P. (1967). Marquage nucleaire par la thymidine tritiee des derives de la crete neurale chez l'amphibien urodele Pleurodeles waltii Macihah. *J. Embryol. Exp. Morphol.* **18**, 343-358.

Concordet, J. P., Lewis, K. E., Moore, J. W., Goodrich, L. V., Johnson, R. L., Scott, M. P. and Ingham, P. W. (1996). Spatial regulation of a zebrafish patched homologue reflects the roles of sonic hedgehog and protein kinase A in neural tube and somite patterning. *Development* **122**, 2835-2846.

Cooper, M. K., Porter, J. A., Young, K. A., Kelley, R. I. and Beachy, P. A. (1998). Plant-derived and synthetic teratogens inhibit the ability of target tissues to respond to Sonic hedgehog signaling. *Science* **280**, 1603-1607.

Cordero, D., Marcucio, R., Hu, D., Gaffield, W., Tapadia, M. and Helms, J. A. (2004). Temporal perturbations in sonic hedgehog signaling elicit the spectrum of holoprosencephaly phenotypes. *J. Clin. Invest.* **114**, 485-494.

Couly, G., Coltey, P. M. and LeDouarin, N. M. (1993). The triple origin of the skull in higher vertebrates: a study in chick-quail chimeras. *Development* **117**, 409-429.

Couly, G., Creuzet, S., Bennaceur, S., Vincent, C. and LeDouarin, N. M. (2002). Interactions between Hox-negative cephalic neural crest cells and the foregut endoderm in patterning the facial skeleton in the vertebrate head. *Development* **129**, 1061-1073.

Crump, J. G., Swartz, M. E. and Kimmel, C. B. (2004a). An integrin-dependent role of pouch endoderm in hyoid cartilage development. *PLOS Biol.* **2**, e244.

Crump, J. G., Maves, L., Lawson, N. D., Weinstein, B. M. and Kimmel, C. B. (2004b). An essential role for Fgfs in endodermal pouch formation influences later craniofacial skeletal pattern. *Development* **131**, 5703-5716.

Cubbage, C. C. and Mabee, P. M. (1996). Development of the cranium and paired fins in the zebrafish Danio rerio (Ostariophysi, Cyprinidae). *J. Morphol.* **229**, 121-160.

David, N., Saint-Etienne, L., Schilling, T. F. and Rosa, F. (2002). Critical requirement for endoderm and FGF in ventral head skeleton induction. *Development* **129**, 263-269.

De Beer, G. R. (1937). *The Development of the Vertebrate Skull*. Oxford: Oxford University Press. Reprinted **1985**, Chicago: Chicago University Press.

Dutton, K. A., Pauliny, A., Lopes, S. S., Elworthy, S., Carney, T. J., Rauch, J., Geisler, R., Haffter, P. and Kelsh, R. N. (2001). Zebrafish colourless encodes sox10 and specifies non-ectomesenchymal neural crest fates. *Development* **128**, 4113-4125.

Ekker, S. C., Ungar, A., R., Greenstein, P., von Kessler, D. P., Porter, J. A., Moon, R. T. and Beachy, P. A. (1995). Patterning activities of vertebrate hedgehog proteins in the developing eye and brain. *Curr. Biol.* **5**, 944-955.

Epperlein, H.-H., Meulemans, D., Brooner-Fraser, M., Steinbeisser, H. and Selleck, M. A. (2000). Analysis of cranial neural crest migratory pathways in axolotol using cell markers and transplantation. *Development* **127**, 2751-2761.

Gorlin, R. J., Cohen, M. M. and Levin, L. S. (1990). *Syndromes of the Head and Neck*. Vol. 1, 3rd edn. New York: Oxford University Press.

Gripp, K. W., Wotton, D., Edwards, M. C., Roessler, E., Ades, L., Meinecke, P., Richieri-Costa, A., Zackai, E. H., Massague, J., Muenke, M. et al. (2000). Mutants in TGIF cause holoprosencephaly and link NODAL signaling to human neural axis determination. *Nat. Genet.* **25**, 205-208.

Hall, B. K. (1980). Tissue interactions and the initiation of osteogenesis and chondrogenesis in the neural crest-derived mandibular skeleton of the embryonic mouse as seen in isolated murine tissues and in recombinations of murine and avian tissues. *J. Embryol. Exp. Morph.* **58**, 251-264.

Helms, J. A., Kim, C. H., Hu, D., Minkoff, R., Thaller, C. and Eichele, G. (1997). Sonic hedgehog participates in craniofacial morphogenesis and is downregulated by teratogenic doses of retinoic acid. *Dev. Biol.* **187**, 25-35.

Horstadius, S. and Sellman, S. (1946). Experimentelle untersuchungen uber die Determination des Knorpeligen Kopfskelettes bei Urodelen. *Nova Acta R. Soc. Scient. Upsal. Ser. 4* **13**, 1-170.

Hu, D. and Helms, J. A. (1999). The role of sonic hedgehog in normal and abnormal craniofacial morphogenesis. *Development* **126**, 4873-4884.

Hu, D., Marcucio, R. S. and Helms, J. A. (2003). A zone of frontonasal ectoderm regulates patterning and growth in the face. *Development* **130**, 1749-1758.

Ingham, P. W. and McMahon, A. P. (2001). Hedgehog signaling in animal development: paradigms and principles. *Genes Dev.* **15**, 3059-3087.

Javidan, Y. and Schilling, T. F. (2004). Development of cartilage and bone. In *Methods in Cell Biology*, Vol. 76 (ed. H. W. Detrich, M. Westerfield and L. I. Zon), pp. 415-436. San Diego: Academic Press.

Jeong, J., Mao, J., Tenzen, T., Kottmann, A. H. and McMahon, A. P. (2004). Hedgehog signaling in the neural crest cells regulates the patterning and growth of facial primordia. *Genes Dev.* **18**, 937-951.

Karlstrom, R. O., Talbot, W. S. and Schier, A. F. (1999). Comparative synteny cloning of zebrafish you-too: mutations in the Hedgehog target gli2 affect ventral forebrain patterning. *Genes Dev.* **13**, 388-393.

Karsenty, G. and Wagner, E. F. (2002). Reaching a genetic and molecular understanding of skeletal development. *Dev. Cell* **2**, 389-406.

Kimmel, C. B., Ballard, W. W., Kimmel, S. R., Ullmann, B. and Schilling, T. F. (1995). Stages of embryonic development in the zebrafish. *Dev. Dyn.* **203**, 253-310.

Kimmel, C. B., Miller, C. T. and Moens, C. B. (2001). Specification and morphogenesis of the zebrafish larval head skeleton. *Dev. Biol.* **233**, 239-257.

Köntges, G. and Lumsden, A. (1996). Rhombencephalic neural crest segmentation is preserved throughout craniofacial ontogeny. *Development* **122**, 3229-3242.

Krauss, S., Concordet, J. P. and Ingham, P. W. (1993). A functionally conserved homolog of the Drosophila segment polarity gene hh is expressed in tissues with polarizing activity in zebrafish embryos. *Cell* **75**, 1431-1444.

Kronenberg, H. M. (2003). Developmental regulation of the growth plate. *Nature* **423**, 332-336.

Landacre, F. L. (1921). The fate of the neural crest in the head of the Urodeles. *J. Comp. Neurol.* **33**, 1-43.

Langille, R. M. and Hall, B. K. (1988). Role of the neural crest in development of the cartilaginous cranial and visceral skeleton of the medaka, Oryzias latipes (Teleostei). *Anat. Embryol.* **177**, 297-305.

Le Douarin, N. M., Creuzet, S., Couly, G. and Dupin, E. (2004). Neural crest plasticity and its limits. *Development* **131**, 4637-4650.

Le Lievre, C. S. (1978). Participation of neural crest-derived cells in the genesis of the skull in birds. *J. Embryol. Exp. Morphol.* **47**, 17-37.

Lumsden, A., Sprawson, N. and Graham, A. (1991). Segmental origin and migration of neural crest cells in the hindbrain region of the chick embryo. *Development* **113**, 1281-1291.

MacDonald, M. E., Abbott, U. K. and Richman, J. M. (2004). Upper beak truncation in chicken embryos with the *cleft primary palate* mutation is due to an epithelial defect in the frontonasal mass. *Dev. Dyn.* **230**, 335-349.

McGonnell, I. M., Clarke, J. D. and Tickle, C. (1998). Fate map of the chick face: analysis of expansion of facial primordia and establishment of the primary palate. *Dev. Dyn.* **212**, 102-118.

Muenke, M. and Beachy, P. A. (2000). Genetics of ventral forebrain development and holoprosencephaly. *Curr. Opin. Genet. Dev.* **10**, 262-269.

Muller, F., Albert, S., Blader, P., Fischer, N., Hallonet, M. and Strahle, U. (2000). Direct action of Nodal-related signal Cyclops in induction of *sonic hedgehog* in the ventral midline of CNS. *Development* **127**, 3889-3897.

Nanni, L., Ming, J. E., Bocian, M., Steinhaus, K., Bianchi, D. W., de Die-Smulders, C., Giannotti, A., Imaizumi, K., Jones, K., Del Campo, M. et al. (1999). The mutational spectrum of the *Sonic Hedgehog* gene in holoprocencephaly: *SHH* mutations cause a significant proportion of autosomal dominant holoprocencephaly. *Hum. Mol. Genet.* **8**, 2479-2488.

Neuhauss, S. C. F., Solnica-Krezel, L., Schier, A. F., Zwartkruis, F., Stemple, D. L., Malicki, J., Abdelilah, S., Stainier, D. Y. R. and Driever, W. (1996). Mutants affecting craniofacial development in zebrafish. *Development* **123**, 357-367.

Nasevicius, A. and Ekker, S. C. (2000). Effective targeted gene 'knockdown' in zebrafish. *Nat. Genet.* **26**, 216-220.

Noden, D. M. (1983). The role of neural crest in patterning of avian cranial skeletal, connective and muscle tissues. *Dev. Biol.* **96**, 144-165.

Odenthal, J. and Nusslein-Volhard, C. (1998). Forkhead domain genes in zebrafish. *Dev. Genes Evol.* **208**, 245-258.

Osumi-Yamashita, N., Ninomiya, Y., Doi, H. and Eto, K. (1994). The contribution of both forebrain and midbrain crest cells to the mesenchyme in the frontonasal mass of mouse embryos. *Dev. Biol.* **164**, 409-419.

Piotrowski, T., Schilling, T. F., Brand, M., Jiang, Y.-J., Heisenberg, C.-P., Beuchle, D., Grandel, H., van Eeden, F. J. M., Furutani-Seiki, M., Granato, M. et al. (1996). Jaw and branchial arch mutants in zebrafish II: anterior arches and cartilage differentiation. *Development* **123**, 345-356.

Roessler, E. and Muenke, M. (2001). Midline and laterality defects: left and right meet in the midline. *BioEssays* **23**, 888-900.

Roessler, E. and Muenke, M. (2003). How a hedgehog might see holoprosencephaly. *Hum Mol. Genet.* **12**, R15-R25.

Roessler, E., Belloni, E., Gaudenz, K., Jay, P., Berta, P., Scherer, S. W., Tsui, L. C. and Muenke, M. (1996). Mutations in the human Sonic hedgehog gene cause holoprosencephaly. *Nat. Genet.* **14**, 357-360.

Schauerte, H. E., van Eden, F. J. M., Fricke, C., Odenthal, J., Strahle, U. and Haffter, P. (1998). Sonic hedgehog is not required for the induction of medial floor plate cells in the zebrafish. *Development* **125**, 2983-2993.

Schilling, T. (1997). Genetic analysis of craniofacial development in the vertebrate embryo. *BioEssays* **19**, 459-468.

Schilling, T. F. and Kimmel, C. B. (1994). Segment and cell type lineage restrictions during pharyngeal arch development in the zebrafish embryo. *Development* **120**, 483-494.

Stone, L. S. (1929). Experiments showing the role of migrating neural crest in the formation of head skeleton and loose connective tissue in Rana palustris. *Roux's Arch.* **118**, 40-77.

Strahle, U., Lam, C. S., Ertzer, R. and Rastegar, S. (2004). Vertebrate floor-plate specification: variations on common themes. *Trends Genet.* **20**, 155-162.

Testaz, S., Jarov, A., Williams, K. P., Ling, L. E., Koteliansky, V. E., Fournier-Thibault, C. and Duband, J.-L. (2001). Sonic hedgehog restricts adhesion and migration of neural crest cells independently of the Patched-Smoothened-Gli signaling pathway. *Proc. Natl. Acad. Sci. USA* **98**, 12521-12526.

Thisse, C., Thisse, B., Schilling, T. F. and Postlethwait, J. H. (1993). Structure of the zebrafish *snail1* gene and its expression in wild-type, *spadetail* and *no tail* mutant embryos. *Development* **119**, 1203-1215.

Trainor, P. A., Ariza-McNaughton, L. and Krumlauf, R. (2002). Role of the isthmus and FGFs in resolving the paradox of neural crest plasticity and prepatterning. *Science* **295**, 1288-1291.

van Eeden, F. J. M., Granato, M., Schach, U., Brand, M., Furutani-Seiki, M., Haffter, P., Hammerschmidt, M., Heisenberg, C.-P., Jiang, Y.-J., Kane, D. A. et al. (1996). Mutations affecting somite formation and patterning in the zebrafish, Danio rerio. *Development* **123**, 153-164.

Varga, Z. M., Amores, A., Lewis, K. E., Yan, Y.-L., Postlethwait, J. H., Eisen, J. S. and Westerfield, M. (2001). Zebrafish smoothened functions in ventral neural tube specification and axon tract formation. *Development* **128**, 3497-3509.

Yan, Y.-L., Miller, C. T., Nissen, R. M., Singer, A., Liu, D., Kirn, A., Draper, B., Willoughby, J., Morcos, P. A., Amsterdam, A. et al. (2002). A zebrafish *sox9* gene required for cartilage morphogenesis. *Development* **129**, 5065-5079.

Zelzer, E. and Olsen, B. R. (2003). The genetic basis for skeletal diseases. *Nature* **423**, 343-348.